

Unconventional Metallic Magnetism in LaCrSb_3

E. Granado^{1,2}, H. Martinho³, M. S. Sercheli³, P. G. Pagliuso⁴, D.D. Jackson^{5,6}, M. Torelli⁵,
J. W. Lynn^{1,2}, C. Rettori³, Z. Fisk⁵, and S. B. Oseroff⁷

¹*NIST Center for Neutron Research, National Institute of Standards and
Technology, Gaithersburg, Maryland 20899*

²*Center for Superconductivity Research, University of Maryland, College
Park, Maryland 20742*

³*Instituto de Física “Gleb Wataghin”, UNICAMP, 13083-970,
Campinas-SP, Brazil*

⁴*Los Alamos National Laboratory, Los Alamos, New Mexico 87545*

⁵*National High Magnetic Field Laboratory, Florida State University,
Tallahassee, Florida 32306*

⁶*Lawrence Livermore National Laboratory, Livermore, California 94550*

⁷*San Diego State University, San Diego, California 92182*

(March 22, 2022)

Abstract

Neutron-diffraction measurements in LaCrSb_3 show a coexistence of ferromagnetic and antiferromagnetic sublattices below $T_C = 126$ K, with ordered moments of $1.65(4)$ and $0.49(4) \mu_B/\text{formula unit}$, respectively ($T = 10$ K), and a spin reorientation transition at ≈ 95 K. No clear peak or step was observed in the specific heat at T_C . Coexisting localized and itinerant spins are suggested.

75.25.+z,61.12.-q,75.40.Cx,65.40.Ba

Typeset using REVTeX

The magnetic exchange mechanisms and spin-correlations mediated by itinerant electrons have attracted renewed interest in the last few years, in part stimulated by the promising technological possibilities of the emerging field of spin electronics [1]. The system of intermetallic antimonides $RCrSb_3$ ($R = \text{La-Nd, Sm, and Gd-Dy}$) crystallizes in a layered orthorhombic structure ($Pbcm$ symmetry), with planes of Sb, R , and a layer of $CrSb_2$, as shown in Fig. 1(a) [2,3]. In this structure, $CrSb_6$ octahedra are connected by face-sharing along **c**, and edge-sharing along **b**. The parent compound, $LaCrSb_3$, has been described as an itinerant ferromagnet [4–6]. The saturation magnetization at low- T (M_{sat}) depends on the sample growth procedure, which is typical of itinerant magnets, and values in the range $0.8 \lesssim M_{sat} \lesssim 1.7 \mu_B/(\text{formula unit, f.u.})$ have been reported [4–8]. The $RCrSb_3$ compounds with $R = \text{Ce, Pr, Nd, and Sm}$ also show a net ferromagnetic (FM) moment from Cr spins below $T_C \sim 105 \text{ K} - 147 \text{ K}$, with possible ordering of the R moments at much lower T [5,7,9,10]. In contrast, the compounds with $R = \text{Gd, Tb, and Dy}$ show no spontaneous FM moment at any temperature [9], indicating a quantum phase transition in this system.

In this paper we report neutron diffraction and specific heat studies on crystals of $LaCrSb_3$ showing $M_{sat} = 1.6 \pm 0.1 \mu_B/\text{f.u.}$ and $T_C \sim 126 \text{ K}$. Neutron diffraction measurements show a coexistence of orthogonal ferromagnetic (FM) and antiferromagnetic (AFM) spin sublattices. A spin-reorientation transition in the bc plane was simultaneously observed for both magnetic sublattices, by either varying T across $T_{sr} \approx 95 \text{ K}$ or by application of small magnetic fields ($H \approx 0.03 \text{ T}$ at 100 K). Also, no clear peak or step in the specific heat was observed at T_C . We suggest a coexistence of localized and itinerant spins in $LaCrSb_3$ to account for these surprising results in a system showing strong metallic magnetism.

The preparation procedure and characterization of the $LaCrSb_3$ samples used in this work are described in ref. [8]. Specific heat measurements on single crystals of typical mass $\sim 5 - 10 \text{ mg}$ were conducted using the relaxation method, with precision better than 1% and accuracy better than 10 % over the studied T -range. dc-magnetization measurements were conducted using a SQUID magnetometer. Neutron diffraction experiments using a crystal weighing $\sim 10 \text{ mg}$ were taken in the $(0kl)$ and $(h0l)$ scattering planes, on BT-2, BT-7, and

BT-9 triple axis spectrometers operated in two-axis mode at the NIST Center for Neutron Research. Pyrolytic graphite monochromators and filters were employed using $\lambda = 2.359(1)$ Å (BT-2 and BT-9) or $\lambda = 2.465(1)$ Å (BT-7), and the collimations before the monochromator, before and after the sample were typically 40' (FWHM). Errors given in parentheses are statistical only, and represent one standard deviation. The magnetic form factor of Cr^{3+} was used in the analysis of the magnetic structure [11]. Field-dependent neutron diffraction measurements were performed using a vertical-field superconducting magnet. A powdered sample was obtained by grinding small crystallites. Neutron powder diffraction measurements were carried out with the BT-9 spectrometer and with the BT-1 high-resolution powder diffractometer at NIST. For measurements with BT-1, monochromatic beams with $\lambda = 1.5402(1)$ Å and $2.0783(1)$ Å were employed. Refinements of the crystal structure of LaCrSb_3 using powder data were carried out with the program GSAS using the following values of the scattering amplitudes: $b(\text{La}) = 0.827$, $b(\text{Cr}) = 0.363$, and $b(\text{Sb}) = 0.564$ ($\times 10^{-12}$ cm) [12]. An orthorhombic model ($Pbcm$ symmetry, see Fig. 1(a)) was employed, with good agreements between observed and calculated intensities at room- T . The refined occupancies are 1 : 0.90(3) : 0.97(2) : 1.00(2) : 0.96(2) for La, Cr, Sb(1), Sb(2), and Sb(3), respectively. The refined atomic positions and displacement factors at room- T do not show significant deviations from those previously reported by Ferguson *et al.* [3] Room- T a , b , and c lattice parameters are 13.2843(5) Å, 6.2119(2) Å, and 6.1191(2) Å, respectively. The T -dependence of lattice parameters and atomic positions does not show any observable lattice anomaly or structural transition between 10 K and 300 K.

Enhancements of some low-angle Bragg reflections due to magnetic ordering were observed by neutron diffraction at low- T . Figure 2(a) shows the T -dependence of the (100) reflection (open circles), as well as a fit to a power law near the transition (solid line), yielding an estimated magnetic ordering temperature $T_C = 126.0(6)$ K. The critical exponent is $\beta = 0.34(2)$. Figure 2(b) shows the T -dependence of the (020) and (002) Bragg reflections. A magnetic intensity, superposed on the nearly constant nuclear intensity, was observed for the (020) reflection below T_C , and is suppressed below $T_{sr} \approx 95$ K. Conversely, the magnetic

intensity of the (002) reflection is suppressed between T_{sr} and T_C and increases below T_{sr} . The magnetic intensities for the (100), (020), and (002) Bragg reflections are due to a FM sublattice. Since the magnetic intensity of a given reflection is sensitive only to the spin projection into the scattering plane [13], the suppression of the (002) magnetic intensity above T_{sr} (see Fig. 2(b)) shows that the FM spins are oriented along the c -axis for $T_{sr} < T < T_C$. Below T_{sr} , the suppression of the (020) magnetic intensity shows that the FM moment is oriented along the b -axis. The FM moment obtained from the diffraction data at 10 K is $M_{FM} = 1.65(4) \mu_B/\text{f.u.}$. This is in very good agreement with $M_{sat} = 1.62 \mu_B/\text{f.u.}$ obtained from bulk magnetization measurements on the same crystal.

Interestingly, $(h, 0, 2l + 1)$ Bragg reflections, with nuclear intensities forbidden by the $Pbcm$ symmetry, were observed below T_C . Such reflections, arising from an AFM spin sublattice, are relatively weak, and could be detected only on the single-crystal. Figure 2(c) shows the T -dependence of the (001) Bragg reflection. Below T_{sr} , this reflection is suppressed, while $(h01)$ Bragg reflections with $h \geq 1$ were still observed (not shown). This is ascribed to a spin reorientation of the AFM sublattice to the c -axis. The ordered AFM moment is $0.49(4) \mu_B/\text{f.u.}$ at 10 K.

To clarify the relationship between the FM and AFM sublattices, neutron diffraction measurements were performed under the application of a magnetic field along the b -axis (H_b) at 100 K. Figures 2(d), 2(e), and 2(f) show the H_b -dependence of the nuclear+FM (100) and (002) and AFM (001) Bragg reflections, respectively. The enhancement of the (002) peak and the constant (100) intensity with field ($H_b \leq 0.05$ T) confirms the expected tendency of the FM sublattice to flop from the c -axis to the direction of H_b . In addition, the suppression of the (001) reflection for $H \gtrsim 0.03$ T (see Fig. 2(f)), with no significant increase of the FM moment in the bc plane (see Fig. 2(d)), and the observation of the (101) AFM reflection up to high magnetic fields (7 T, not shown), shows that the AFM sublattice flops to the c -axis for a small field along b . The synchronized reorientation of the FM and AFM sublattices, by varying either T or H_b , reveals that the AFM moment is orthogonal to the FM moment. This result does not support a FM+AFM inhomogeneous magnetic state for

LaCrSb₃, because in this scenario the AFM domains are not expected to couple with small magnetic fields [14]. In contrast, a non-collinear canted spin arrangement trivially explains the orthogonality between the FM and AFM sublattices. The spin structures that account for the observed magnetic intensities of the (100), (020), (002) and (*h*01) ($0 \leq h \leq 7$) reflections at 10 K ($\chi^2 = 1.7$) and 110 K ($\chi^2 = 1.1$) are illustrated in Fig. 1(b). The total ordered magnetic moment is 1.72(5) μ_B /f.u. at 10 K, translating into 1.91 μ_B /Cr for 90 % Cr occupancy. The results above do not exclude the possibility of an inhomogeneous canted state, such as proposed for lightly Ca-doped LaMnO₃ [15]. Neutron scattering can be used to investigate the possible inhomogeneities below T_C and spin correlations above T_C in LaCrSb₃, when larger crystals become available.

The magnetic state above T_C was investigated by means of specific heat measurements. Figure 3 shows the specific heat, $C(T, H = 0)$, and the *dc*-magnetization, $M(T, H_b = 1$ kOe), measured on the same crystal. Remarkably, neither a peak or step was observed in $C(T_C)$, within the resolution of our experiment, which was reproduced for several crystals and different equipments. To illustrate the significance of this result, the solid line in Fig. 3(a) shows a simulated magnetic contribution, $C_{mag}^{simul}(T)$, with a Gaussian distribution for $C_{mag}^{simul}(T)/T$ with full-width at half-maximum of 20 K and area given by the entropy of the ideal paramagnetic state for spin-1, $S_{PM} = 9.1$ J/Kmol. The experimental $C(T)$ curve indicates that no measurable change in the magnetic entropy takes place at $T \approx T_C$, despite the relatively sharp magnetic ordering transition observed by magnetization and neutron-diffraction. Analyses of $C(T)$ curves commonly yield magnetic entropies above T_C smaller than expected for the paramagnetic state, mostly due to magnetic correlations at $T > T_C$ and the difficulty of separating the phononic from the spin-wave specific heats at $T < T_C$. Nonetheless, the absence of any clear feature in the specific heat of LaCrSb₃ at T_C is striking, given the large ordered magnetic moments. This result indicates magnetic correlations above T_C which are unusually strong and possibly extended in range. Such correlations might be low-dimensional in character due to the layered crystal structure of this compound (see Fig. 1(a)). On the other hand, the critical exponent below T_C obtained from neutron-diffraction,

$\beta = 0.34(2)$ (see Fig. 2(a)), is indicative of three-dimensional spin fluctuations, at least in the ordered phase. The magnetic susceptibility in the powdered sample (not shown) could be fit by the relation $\chi = \chi_0 + C/(T - \Theta_{CW})$ between ~ 200 K and 800 K [4], with $\chi_0 = -0.0020$ emu/mol(f.u.), $C = 1.13$ Kemu/mol(f.u.), and $\Theta_{CW} = 145$ K. Nonetheless, for a fairly large T -interval, between $T_C = 126$ K and ~ 200 K, a clear deviation from this behavior was observed (see also refs. [4,8]). This is not surprising in view of the strong spin correlations above T_C inferred from our specific heat study.

The coexistence of FM and AFM sublattices observed in LaCrSb_3 is very unusual in itinerant magnetic systems, which typically show either purely FM or spin-density-wave AFM spin structures. Nor is it common in insulating compounds with the spins on transition-metal ions, where the magnetic properties are described in good approximation by the isotropic Heisenberg Hamiltonian, and a spiral ground state is the general solution for equivalent spins [16]. We should mention that anisotropy terms in the spin Hamiltonian, originated from spin-orbit coupling, might give rise to canted spin structures such as those drawn in Fig. 1(b). However, we emphasize that these terms are typically very small compared to isotropic exchange for transition-metal compounds, and thus the large angle between neighboring Cr spins, $36(4)^\circ$, is not a result of spin anisotropy. On the other hand, anisotropy forces must be considered to understand the abrupt spin reorientation transition at 95 K. This phenomenon is commonly observed in compounds with competing spin anisotropies from different magnetic ions, or from the same element at distinct crystallographic sites. However, in LaCrSb_3 , the Cr ions are placed at the same site. Also, the spins remain oriented in the same plane at T_{sr} (see Fig. 1(b)), thus antisymmetric Dzialoshinski-Moriya exchange is not the driving force of this transition. This indicates at least two species of magnetic electrons in LaCrSb_3 with distinct and competing symmetric anisotropies.

We thus suggest a coexistence of localized and itinerant spins in LaCrSb_3 . The highly anisotropic crystal structure of LaCrSb_3 may lead to distinct Cr $3d$ orbitals showing largely different degrees of hybridization with the Sb states, and therefore different sub-band dispersions. This seems to be consistent with the spike found close to the Fermi level in the

calculated Cr contribution to the density of states of LaCrSb_3 [4]. As discussed by Korotin *et al.* for the possibly similar case of CrO_2 [17], the least hybridized sub-band, having almost pure Cr:3d character, is more sensitive to the on-site Coulomb repulsion, and tends to become localized. The itinerant spins, from the most hybridized Cr-(Sb(1),Sb(2)) sub-band, may then polarize the localized spins, leading to a FM real-charge-transfer exchange mechanism which is closely related to the double-exchange [18]. We note that the electronic transport in LaCrSb_3 is very sensitive to the magnetic order. In fact, the interlayer resistivity shows a peak at T_C [8], while the resistivity measured along **b** and **c** is similar to calculated curves in the double-exchange model [19], showing metallic behavior with a change of concavity at T_C [8].

This picture offers insight into the results presented here. At room- T , the Cr-Sb-Cr bonding angles are between $68.3(2)^\circ$ and $68.8(2)^\circ$ for neighboring Cr ions along **c**, $93.2(2)^\circ$ along **b**, and $133.9(2)^\circ$ along [011] (see Fig. 1), leading to superexchange interactions of different magnitudes, and possibly different signs. In addition, a significant Cr-Cr direct bonding [2,4] may give rise to an additional AFM coupling along **c**. When such exchange mechanisms, represented by an isotropic Heisenberg spin Hamiltonian, compete with real-charge-transfer exchange, a coexistence of FM and AFM sublattices, such as observed in LaCrSb_3 , can occur. Very recently, Solovyev and Terakura proposed that either canted spins or FM+AFM phase-separated states may be stabilized as a result of such a competition in manganites [20]. The unusually strong spin correlations in the disordered phase for LaCrSb_3 , inferred from the specific heat results, suggest that the localized moments are polarized by the itinerant spins even above T_C .

In conclusion, we report unconventional metallic magnetism and suggest a coexistence of localized and itinerant spins in LaCrSb_3 . Whether the itinerant spins are also responsible for the low- T ordering of the R spin sublattice and the magnetic quantum phase transition in other members of the $R\text{CrSb}_3$ series [5,7,9,10] is likely, but confirmation requires more detailed studies.

We thank M. F. Hundley and J. D. Thompson for helpful discussions. This work was

supported by FAPESP and CNPq, Brazil, NSF-MRSEC, DMR 00-80008, NSF DMR 01-02235 and NSF DMR 99-71348, USA.

REFERENCES

- [1] see, for example, S. A. Wolf *et al.*, Science **294**, 1488 (2001).
- [2] M. Brylak and W. Jeitschko, Z. Naturforsch. **50b**, 899 (1995).
- [3] M.J. Ferguson, R.W. Hushagen, and A. Mar, J. Alloys Comp. **249**, 191 (1997).
- [4] N.P. Raju *et al.*, Chem. Mater. **10**, 3630 (1998).
- [5] M.L. Leonard, I.S. Dubenko, and N. Ali, J. Alloys Comp. **303**, 265 (2000).
- [6] I.S. Dubenko, P. Hill, and N. Ali, J. Appl. Phys. **89**, 7326 (2001).
- [7] K. Hartjes, W. Jeitschko, and M. Brylak, J. Magn. Magn. Mater. **173**, 109 (1997).
- [8] D.D. Jackson, M. Torelli, and Z. Fisk, Phys. Rev. B **65**, 014421 (2001).
- [9] M. Leonard, S. Saha, and N. Ali, J. Appl. Phys. **85**, 4759 (1999).
- [10] L. Deakin *et al.*, Chem. Mater. **13**, 1407 (2001).
- [11] P.J. Brown in: *International Tables for Crystallography*, Ed. A.J.C. Wilson, Vol. C, pp. 391, Kluwer Academic Publishers, 1995.
- [12] C. Larson and R.B. Von Dreele, Los Alamos National Laboratory Report No. LAUR086-748, 1990 (unpublished).
- [13] see, for example, G.E. Bacon, *Neutron Diffraction* (Oxford, Bristol, 1975).
- [14] E.O. Wollan and W.C. Koehler, Phys. Rev. **100**, 545 (1955).
- [15] M. Hennion *et al.*, Phys. Rev. Lett. **81**, 1957 (1998).
- [16] J.B. Goodenough, *Magnetism and the Chemical Bond* (John Wiley, New York, 1963), pp. 131-137, and references therein.
- [17] M.A. Korotin *et al.*, Phys. Rev. Lett. **80**, 4305 (1998).
- [18] C. Zener, Phys. Rev. **82**, 403 (1951).

[19] see, for example, S. Ishizaka and S. Ishihara, Phys. Rev. B **59**, 8375 (1999).

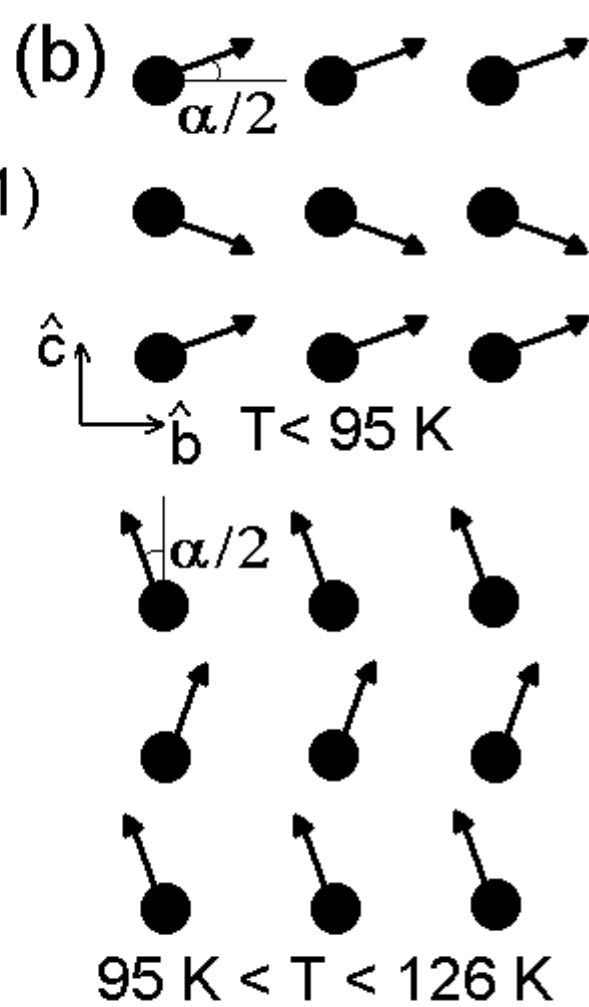
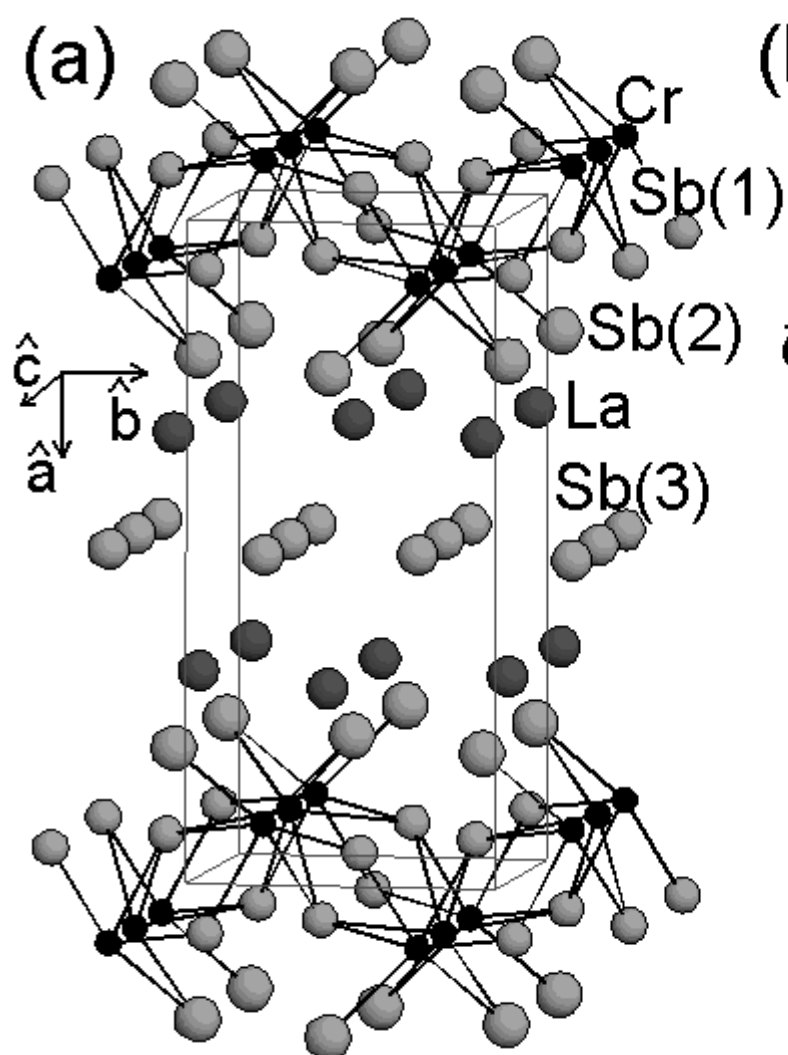
[20] I. V. Solovyev and K. Terakura, Phys. Rev **63**, 174425 (2001).

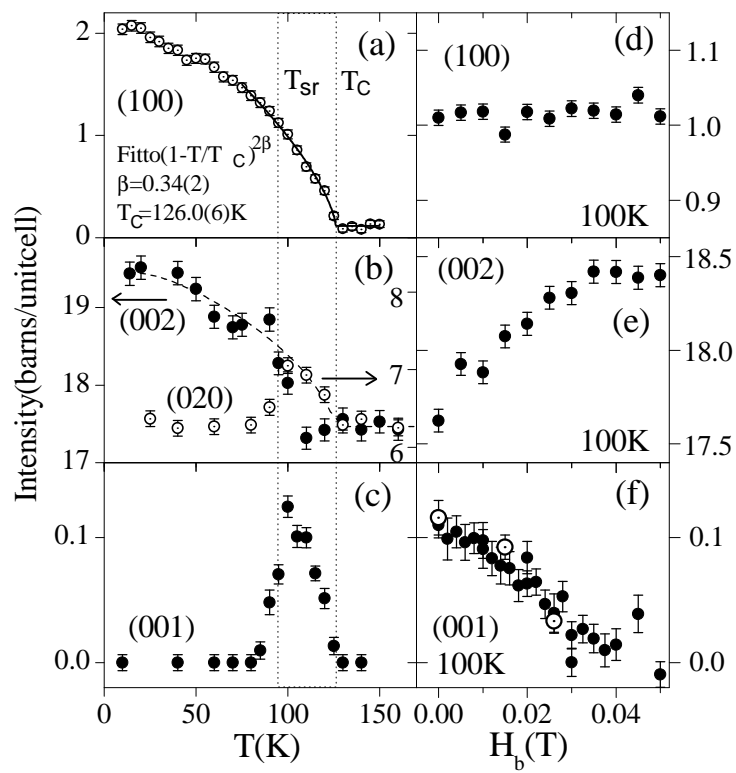
FIGURES

FIG. 1. (a) Crystal structure of LaCrSb_3 . (b) Projection of the Cr sublattice onto the \mathbf{bc} plane. The arrows represent the Cr magnetic structures in this compound below 95 K (T_{sr}) and between T_{sr} and 126 K (T_C). The angle between neighboring spins, $\alpha = 36(4)^\circ$, is the same within experimental error for both T -intervals.

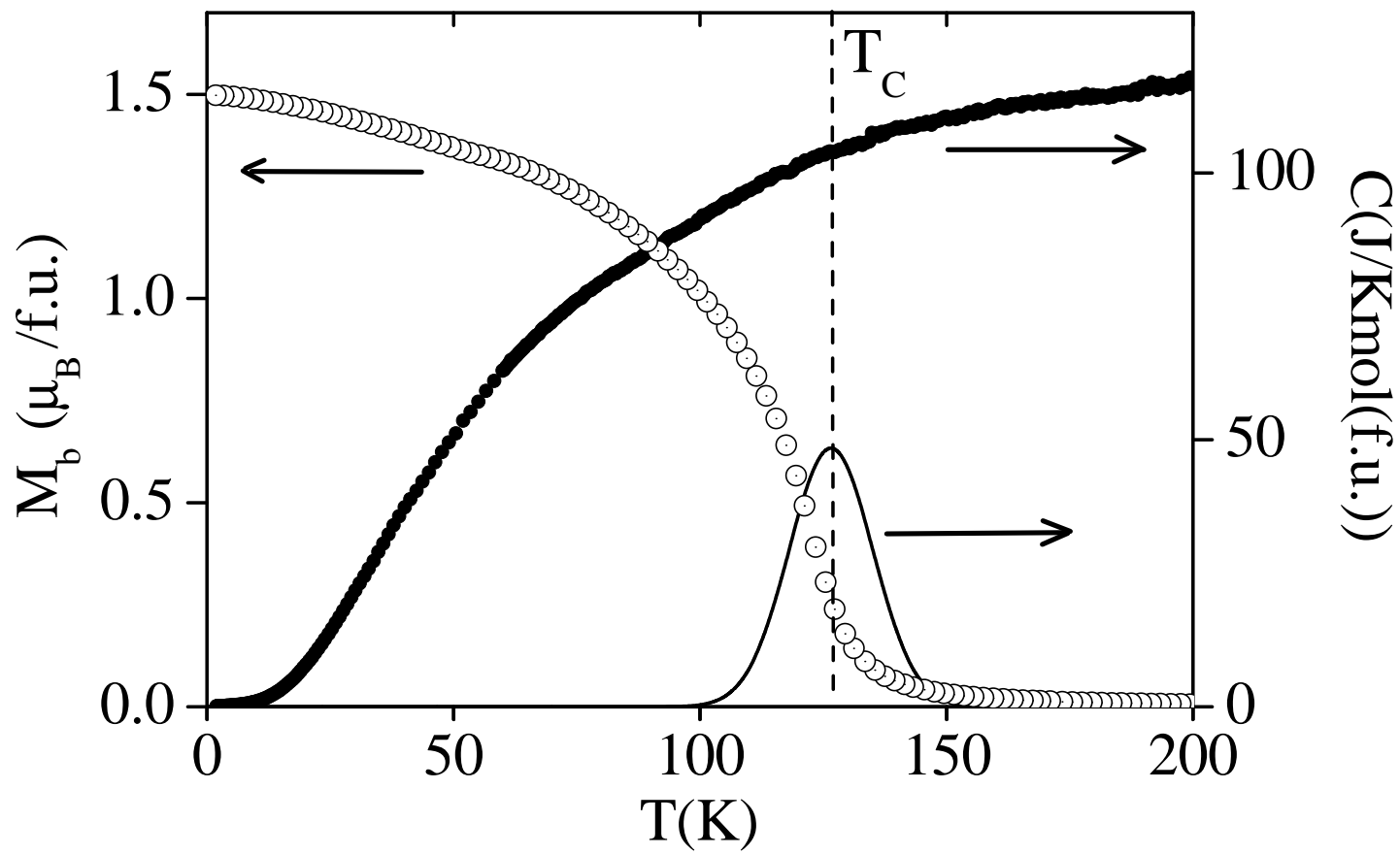
FIG. 2. (a-c) T -dependence of the intensities of selected Bragg reflections: (100) (a), (020) and (002) (b), and (001) (c). The solid line in (a) is a fit to a power law. The dashed line in (b) is a guide to the eyes. The vertical dotted lines mark the spin reorientation (T_{sr}) and long-range magnetic ordering (T_C) transition temperatures. (d-f) Magnetic-field-dependence of the intensity of (100) (d), (002) (e), and (001) (f) reflections at 100 K, taken with increasing field (filled symbols), and with decreasing field after the application of 0.035 T (open symbols in (f)). The field was applied along \mathbf{b} .

FIG. 3. T -dependence of the dc -magnetization (open symbols) and zero-field specific heat, $C(T)$ (filled symbols), measured for the same crystal of LaCrSb_3 . The magnetization was measured under an applied magnetic field of 0.1 T along \mathbf{b} . The solid line is a simulation for the magnetic contribution to $C(T)$ (see text).





Granadoetal.,Fig.2



Granadoetal.,Fig.3